AGU PUBLICATIONS

Geophysical Research Letters

RESEARCH LETTER
10.1002/2016GL071921

Key Points:
- We identify a robust vertical gradient of projected soil moisture changes under global warming with more negative changes near the surface
- We interpret this gradient as resulting from the physical asymmetry between winter precipitation/infiltration and summer evaporation
- These results shed light on the discrepancy between projected land aridity increase and more modest changes in the surface water budget

Supporting Information:
- Supporting Information S1

Correspondence to:
A. Berg,
ab5@princeton.edu

Citation:
Berg, A., J. Sheffield, and P. C. D. Milly (2017), Divergent surface and total soil moisture projections under global warming, *Geophys. Res. Lett.*, *44*, 236–244, doi:10.1002/2016GL071921.

Received 10 NOV 2016
Accepted 28 DEC 2016
Accepted article online 30 DEC 2016
Published online 13 JAN 2017

Divergent surface and total soil moisture projections under global warming

Alexis Berg[1], Justin Sheffield[1,2], and P. C. D. Milly[3]

[1]Department of Civil and Environmental Engineering, Princeton University, Princeton, New Jersey, USA, [2]Geography and Environment, University of Southampton, Southampton, UK, [3]U.S. Geological Survey, and NOAA/Geophysical Fluid Dynamics Laboratory, Princeton, New Jersey, USA

Abstract Land aridity has been projected to increase with global warming. Such projections are mostly based on off-line aridity and drought metrics applied to climate model outputs but also are supported by climate-model projections of decreased surface soil moisture. Here we comprehensively analyze soil moisture projections from the Coupled Model Intercomparison Project phase 5, including surface, total, and layer-by-layer soil moisture. We identify a robust vertical gradient of projected mean soil moisture changes, with more negative changes near the surface. Some regions of the northern middle to high latitudes exhibit negative annual surface changes but positive total changes. We interpret this behavior in the context of seasonal changes in the surface water budget. This vertical pattern implies that the extensive drying predicted by off-line drought metrics, while consistent with the projected decline in surface soil moisture, will tend to overestimate (negatively) changes in total soil water availability.

1. Introduction

Understanding the response of the terrestrial water cycle to global warming is critical to anticipate impacts on water resources, agriculture, and ecosystems. Although land precipitation is projected to increase slightly, on average, with climate change, many studies indicate that as the Earth gets warmer, climatic aridity over land will increase [*Feng and Fu*, 2013; *Scheff and Frierson*, 2015; *Fu and Feng*, 2014; *Lin et al*., 2015; *Zhao and Dai*, 2015; *Huang et al*., 2016] and droughts will become more intense and widespread [*Burke et al*., 2006; *Dai*, 2013; *Cook et al*., 2014; *Zhao and Dai*, 2015]. Such studies typically rely on aridity or drought indices, such as the aridity index or the Palmer Drought Severity Index (PDSI), which are essentially supply/demand metrics comparing changes in precipitation (atmospheric supply of water to the land surface) to estimates of changes in potential evapotranspiration (PET; considered as the atmospheric water demand exerted on the land). These metrics are off-line diagnostics calculated a posteriori from climate model outputs, using near-surface atmospheric variables. PET is often calculated, for instance, with the Penman-Monteith equation, which combines model outputs of near-surface temperature, wind speed, relative humidity, and radiation. From a global perspective, the widespread drying of the land surface identified in the studies above is generally interpreted as the result of the dominant, ubiquitous PET increase caused by warming-induced increase in vapor pressure deficit (VPD) and increased net radiation [e.g., *Scheff and Frierson*, 2014], which overwhelms the slight overall precipitation increase projected over land [e.g., *Zhao and Dai*, 2015].

Recent research, however, suggests that projections based on off-line aridity and drought metrics may intrinsically overestimate future increase in droughts and decrease in water availability [*Hoerling et al*., 2012; *Roderick et al*., 2015; *Milly and Dunne*, 2016; *Swann et al*., 2016]. These metrics, for instance, do not account for reduced plant stomatal conductance associated with increased atmospheric CO_2, which *Milly and Dunne* [2016] show will reduce projected PET increases in the future. *Milly and Dunne* [2016] further show that fundamental differences between the nature of climate model outputs and the input requirements of drought or aridity metrics (which were originally meant as monitoring diagnostics to be computed from observations) lead to overestimation of future PET trends. Finally, computing metrics offline, based on climate model outputs, may introduce inconsistencies if used with impact models (e.g., crop and hydrological models). For instance, climate model outputs already reflect land surface and plant feedbacks on near-surface climate (e.g., temperature and relative humidity), which have been shown to amplify aridity increases [*Berg et al*., 2016]; thus, use of climate model outputs in off-line models may double-count land surface and plant feedbacks, leading to overestimates of future stress [*Swann et al*., 2016]. As a result, these studies argue that,

instead of relying upon off-line metrics focusing on conditions of the near-surface atmosphere, projections of future aridity should be directly based on actual changes in the variables of the terrestrial water cycle simulated by climate models, such as changes in precipitation, evapotranspiration, runoff, and soil moisture [e.g., *Milly et al*., 2005; *Sheffield and Wood*, 2008].

Most existing analyses of future soil moisture changes from climate model projections show widespread decreases in soil wetness, with no regions displaying significant increases [*Collins et al*., 2013; *Zhao and Dai*, 2015]. Such projections appear to support PDSI and aridity projections of increased land drying. However, such analyses, including the one displayed in the Fifth Assessment Report Intergovernmental Panel on Climate Change report [*Collins et al*., 2013], focus mostly on surface (upper 10 cm) soil moisture. Indeed, surface soil moisture is provided by all climate models and more readily comparable among models than the total (full soil column) variable, which reflects differences across models in terms of, e.g., soil depth, layering, and hydraulic parameters. We suggest, however, that a diagnosis based on surface soil moisture may remain incomplete, both in terms of understanding global changes in the water cycle, as well as inferring impacts on water resources for agriculture and ecosystems. Many vegetation types, for instance, can typically access moisture down to 2–3 m [e.g., *Canadell et al*., 1996]. While total soil moisture changes have sometimes been analyzed separately [*Wang*, 2005; *Sheffield and Wood*, 2008], we argue that a more systematic, comprehensive examination of soil moisture projections at different depths from climate models is needed. Here we examine surface, total, and layer-by-layer soil moisture changes projected by climate models from the Coupled Model Intercomparison Project phase 5 (CMIP5).

2. Data and Methods

2.1. CMIP5 Outputs

We use soil moisture outputs for total soil moisture, surface (upper 10 cm) soil moisture, and soil moisture by layer from CMIP5 models (respectively, variables mrso, mrsos, and mrlsl in the CMIP5 archive) for the historical simulations over 1976–2005 (present) and for projections following the Representative Concentration Pathway version 8.5 emission scenario over 2070–2099 (future). Among the CMIP5 ensemble, 25 models provided all three variables for both simulations (see list in Table S1 in the supporting information). We use monthly outputs and compute annual means, as well as June-July-August and December-January-February averages to investigate summer versus winter changes in both hemispheres.

2.2. Comparison of Projections

The details of the models' soil schemes vary widely. In our ensemble, hydrologically active soil depth in the models varies from 3 to 14 m and the number of soil layers from 3 to 23 (see Table S1). The hydraulic properties of soils will also vary among models. As a result, while the average surface soil moisture provided by models is quantitatively comparable, total soil water content varies widely: for instance, the maximum monthly total soil water content over the hydrologically active layers (across pixels and over the historical period) is found to vary from nearly 1400 kg/m^2 in model ACCESS1-0 to 7000 kg/m^2 in MIROC-ESM. In that context, comparing absolute changes in total soil moisture between models is not robust, as changes of similar magnitudes may have different implications in terms of water stress in different models. We thus compare changes in soil moisture as the fraction (%) of present-day simulated mean. To account for differences in variability (i.e., how a long-term change compares to present-day interannual fluctuations), we also compute changes in standardized anomalies, where future-minus-present differences are normalized by the interannual standard deviation of present-day simulated soil moisture [e.g., *Koster et al*., 2009]. To compute multimodel means and uncertainties, all variables were regridded on a $2° \times 2°$ grid before calculating changes.

It can be argued that model soil schemes going down to 3 m versus 14 m fundamentally do not seek to represent the same processes; further, in the context of changes in terrestrial water resources we are more interested in changes occurring over parts of the soil column mostly accessible to ecosystems, i.e., the top few meters. In that context, we use soil moisture outputs by layers as provided by the climate models to compute a 3 m soil moisture variable, i.e., soil moisture integrated down to 3 m (3 m corresponds to the maximum soil depth in a number of models). Soil moisture outputs by layer were also linearly interpolated to a common vertical profile so that a multimodel average vertical profile could be computed. Based on the diversity of model vertical profiles, we chose the common vertical levels to be 0.05, 0.22, 0.68, and 2 m (with bounds

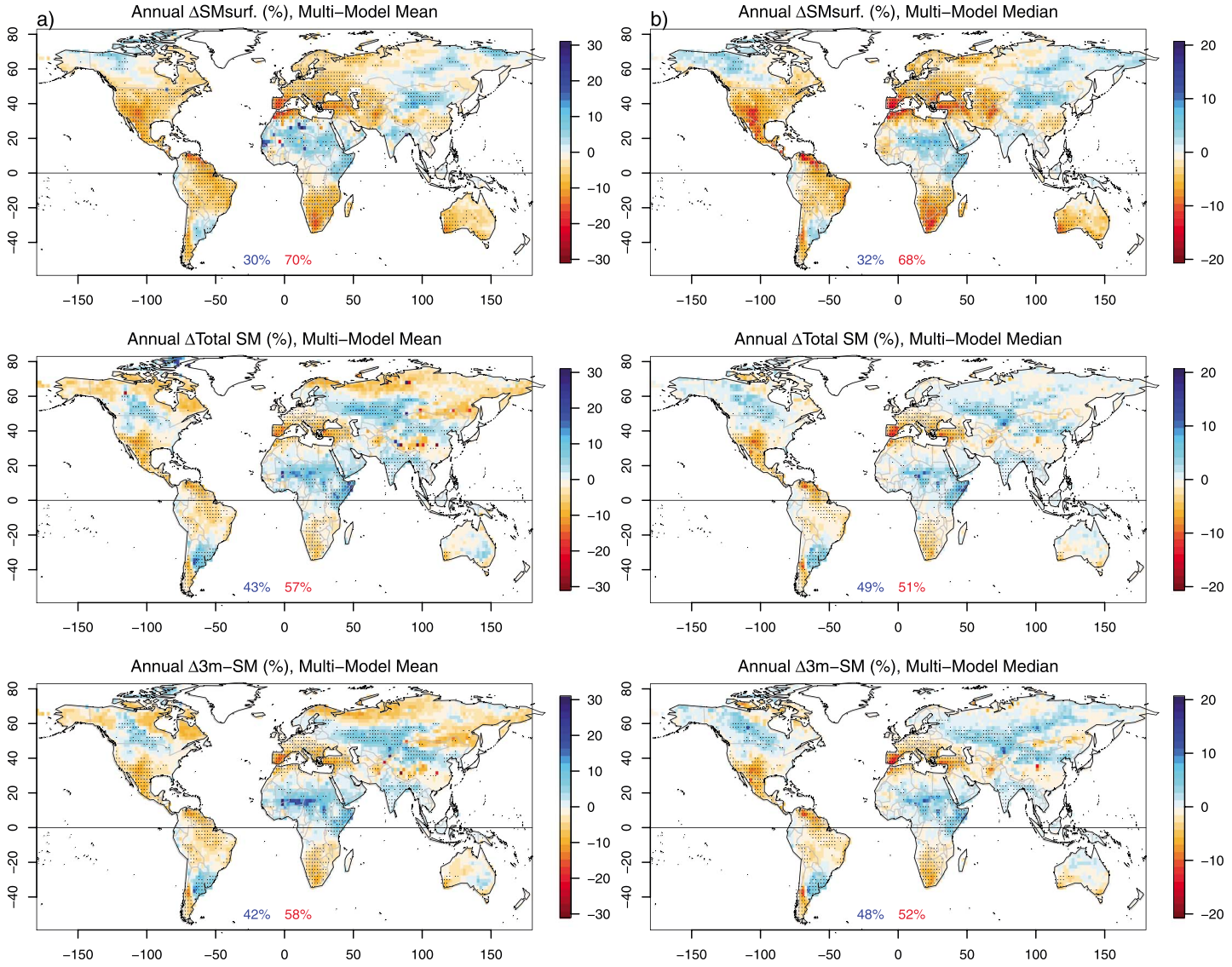

Figure 1. (a) Multimodel annual mean change between 1976–2005 and 2070–2099 (using RCP8.5 scenario) of (top to bottom) surface (upper 10 cm) soil moisture (SM), total SM, and SM integrated down to 3 m. Values are percentages of simulated present-day values. (b) Same as in Figure 1a with multimodel median. On all plots, the numbers indicate the share of the land surface with positive (blue) or negative (red) changes. The stippling indicates where more than three quarters of the models agree on the sign of the projected change.

at 0, 0.1, 0.35, 1, and 3 m). Note that with this profile, the first layer corresponds to the surface (upper 10 cm) "mrsos" variable used in other studies [e.g., *Zhao and Dai*, 2015].

3. Results

Figure 1a shows the multimodel mean projections of change in annual surface, total, and 3 m soil moisture between 1976–2005 and 2070–2099. Results for surface soil moisture are equivalent to those in the literature [e.g., *Collins et al.*, 2013; *Zhao and Dai*, 2015]. They feature large-scale drying of surface soils over most of North America, South America, Europe extending in northern and central Asia and the Middle East, southern Africa, and Australia. Overall, 70% of the land surface (excluding Greenland and Antarctica) displays negative changes based on the multimodel mean in Figure 1a. In contrast, projections of negative changes in total soil moisture are more muted, in both extent and amplitude (57% of the land surface displays negative changes). Regions of negative changes (e.g., southern U.S. and Central America, northern South America,

Mediterranean region, and South Africa) display relative changes of reduced amplitude compared to surface changes. Some regions that show projected decreases (or little change) in surface soil moisture show increases in mean total soil moisture: northern U.S. and central Canada and central Asia. Changes in 3 m soil moisture are largely similar to those in total soil moisture, indicating that relative changes in soil moisture below 3 m are approximately the same as relative changes of 3 m soil moisture (in the models where soils extend below 3 m).

Figure 1b shows the same projections as in Figure 1a but for the multimodel median. For surface soil moisture, the multimodel mean and median are largely similar, indicating that the distribution of model changes is not skewed by stronger changes in a few models. For total and 3 m soil moisture, on the other hand, the mean and median changes differ strongly at high latitudes; Figure S1 in the supporting information confirms that the spread in soil moisture changes is greatest in these regions. In particular, large areas of negative changes in the multimodel mean are not present in the multimodel median, indicating that the former signal is dominated by strong relative decrease in total soil moisture in a few models. We point out that all soil moisture variables considered here include both liquid and frozen soil moisture. At high latitudes, a large, but variable, portion of soil moisture, across models, is frozen; permafrost is robustly projected to decrease with global warming, but the details of simulating permafrost vary between models, and the amplitude of this decrease displays a large spread (Figure S2) [e.g., *Koven et al*., 2013]. Given the similarity of patterns in Figures 1 and S2 at high latitudes, we interpret the skewed projections of total soil moisture changes at high latitudes as reflecting the spread in projected changes in permafrost. We point out that, conceptually, permafrost degradation may not imply increased water stress: the decrease in soil moisture in these regions may be interpreted as the remobilization of long-term frozen soil moisture; converted to liquid soil water; and then lost to either evaporation, drainage, or runoff, in association with local simulated changes in vegetation [*Lawrence et al*., 2015].

Figure S3 shows the changes expressed in standardized anomalies. Negative changes in surface or total soil moisture over regions such as the Mediterranean basin appear typically a few times larger than the interannual variability over the present climate, indicating that the changes in Figure 1 are meaningful compared to model variability. For total or 3 m soil moisture, changes in regions where total soil moisture variability is low are magnified, such as in deserts or over permafrost regions.

Figure 1 shows that consideration of soil moisture below the upper 10 cm qualitatively changes the picture of projected changes in soil water content. Figure 1 also implies that changes in soil moisture vary with depth. Figure 2 confirms this by showing mean latitude versus depth projections of soil moisture changes. Despite large quantitative uncertainties between models in terms of relative changes at various depths/latitudes, Figure 2 reveals a number of robust qualitative features. First, in regions where both surface and deeper soil moisture changes are negative on average (e.g., around 30–40°N and 10–20°S), there tends to be a vertical gradient in the amplitude of these changes, with more negative changes near the surface and changes of decreasing amplitude with depth. Second, in regions where on average both surface and deeper soil moisture are projected to increase (e.g., around 10–20°N), the changes of greatest amplitude take place below the surface. Finally, there are latitudinal regions (e.g., 40–60°N and 30–40°S) where projections suggest that surface soils could dry while soil moisture increases deeper down. These are the same regions featuring contrasted projections of upper 10 cm soil moisture versus total soil moisture in Figure 1: central northern U.S. and Canada and central Asia. Note that Figure 2 shows the changes in volumetric soil moisture: when accounting for the depths of the different layers, changes in total water amounts are greater deeper down. This explains the positive total changes in these regions in Figure 1.

As a first-order, global diagnosis, Figure 2 conflates slightly different longitudinal responses. Figure S4 confirms the patterns described above in more details by focusing on three different longitudinal bands with more homogeneous zonal changes, showing that the vertical gradient in Figure 2 is not due to zonal averaging. Figure S4 also highlights the contrasting changes in soil moisture, also evident in Figure 1, between Central America and the rest of tropical land (e.g., tropical Africa).

Finally, changes north of 60°N in Figure 2 appear inconsistent across models, as demonstrated by the qualitative difference in the multimodel median and mean projected changes. As mentioned above, this inconsistency likely corresponds to uncertainties in the simulation of permafrost degradation and fate of the associated meltwater.

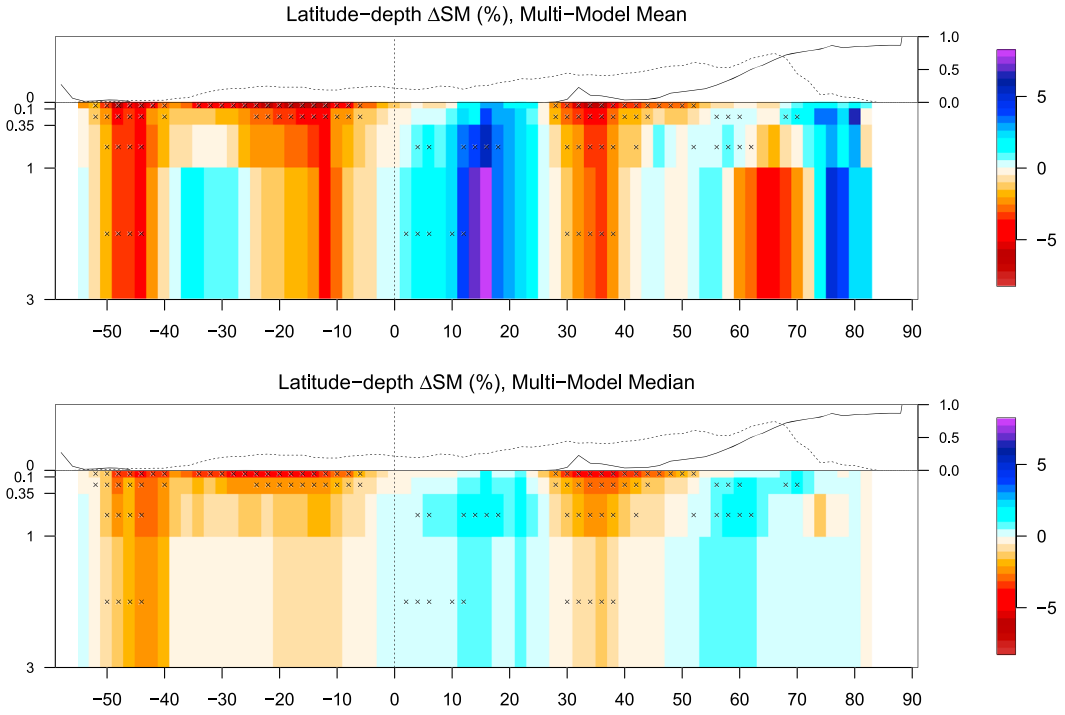

Figure 2. Multimodel (top) mean and (bottom) median relative change (%) in volumetric soil moisture between 1976–2005 and 2070–2099 as a function of depth (left-hand *y* axis (m)) and latitude (*x* axis). The stippling indicates where more than three quarters of the models agree on the sign of projected changes. The full line represents the multimodel mean ratio of frozen over total soil moisture from Figure S2; the dotted line represents the global fraction of land by latitude (for both lines, values are on the right-hand *y* axis).

4. Discussion

Overall, Figures 1 and 2 show that there is a vertical gradient in projected soil moisture changes: changes are more negative near the surface and less negative, or even of opposite sign, under the surface, to depths of a couple meters. Because of this gradient, changes in surface soil moisture appear more negative than diagnoses based on total or 3 m soil moisture.

As has been noted in previous studies [*Dai*, 2013; *Zhao and Dai*, 2015], projected changes in upper 10 cm soil moisture (Figure 1) appear largely similar to changes in aridity and drought metrics (e.g., *P*/PET and PDSI [*Dai*, 2013; *Fu and Feng*, 2014; *Cook et al.*, 2014; *Zhao and Dai*, 2015]), lending support to the associated projections of increased continental drying. A major feature noted in these studies is that the projected land drying expands beyond the more limited regions of projected reduced mean precipitation (see Figure 3), in particular in the Northern Hemisphere (NH) middle and high latitudes [*Cook et al.*, 2014]. This expansion is attributed to the globally extensive increases in PET, which exerts a drying influence on the land surface: increased PET not only intensifies drying in areas where precipitation is already reduced but also causes drying in regions that otherwise experience positive precipitation trends [e.g., *Cook et al.*, 2014].

Figure 3 is consistent with the foregoing argument to the extent that it shows, in summer in NH middle and high latitudes, changes in evapotranspiration (*E*) to be more positive (or less negative) than changes in precipitation (*P*), resulting in a large negative *P-E* anomaly in these regions. This anomaly is consistent with a decrease in soil moisture. However, Figure 4 shows that the associated summertime soil drying predominantly affects upper surface soil moisture; it is less reflected in changes in soil moisture availability going down to a couple of meters. We interpret this gradient as reflecting the fact that *E* extracts water preferentially from the upper tens of centimeters of the soil column, which are directly affected by both soil evaporation and plant transpiration, whereas deeper levels, with generally lower root density, are subject only to a small portion of the transpiration. Drying of these upper layers of soil does not readily spread to

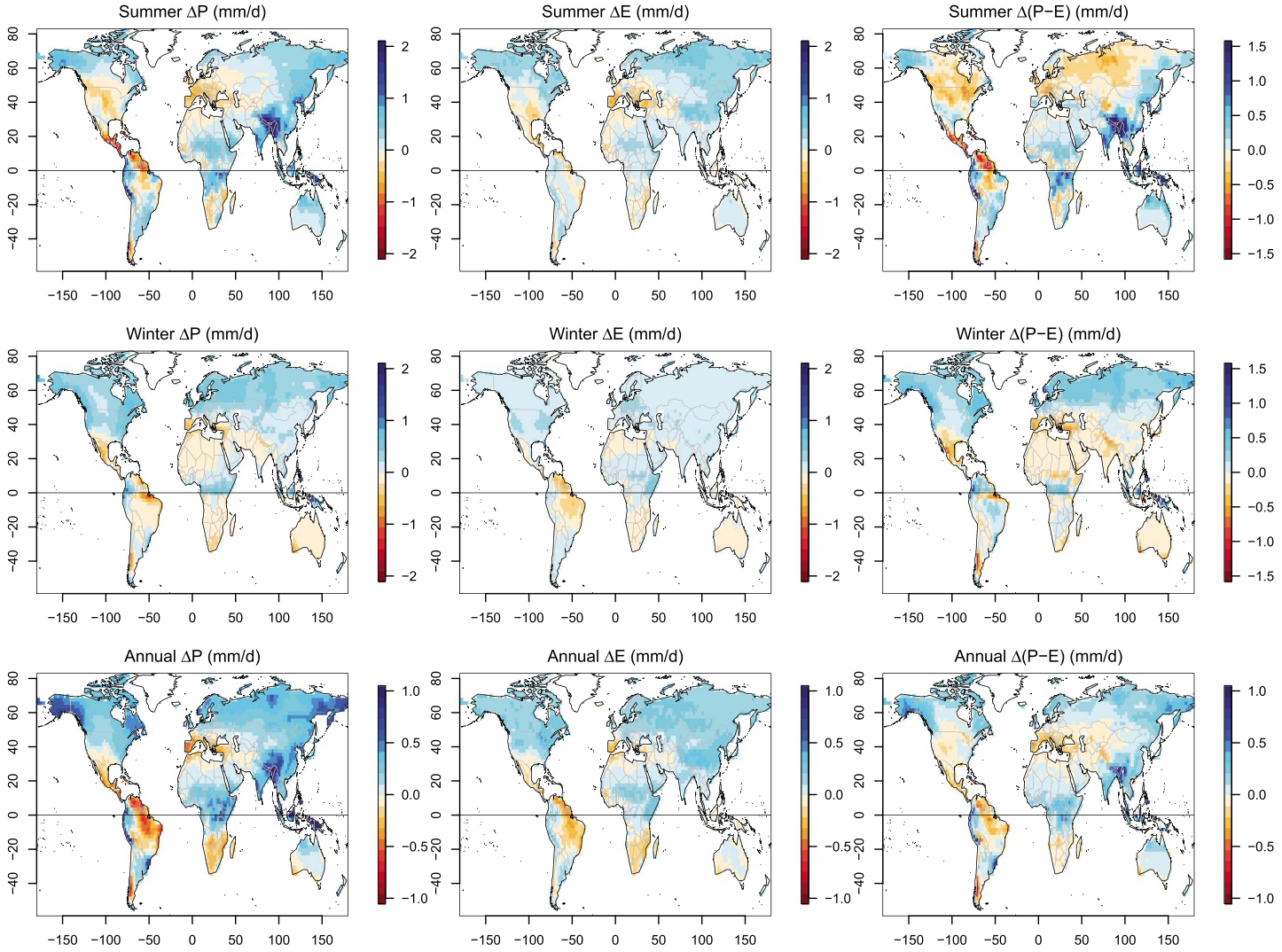

Figure 3. Multimodel mean change in (top) summer, (middle) winter, and (bottom) annual (left) precipitation *P* (mm/d), (middle) evapotranspiration *E* (mm/d), and (right) *P-E* (mm/d). Summer and winter are defined in each hemisphere; i.e., summer is JJA in the Northern Hemisphere and DJF in the Southern Hemisphere, and winter is DJF and JJA, respectively. Note that for all these quantities, multimodel mean and median changes are nearly identical. The colors saturate for values beyond the color-scale limits (e.g., for *P* changes over the Himalayas). Note the different scales for various plots.

deeper layers, because upward capillary flow from below is a relatively slow process. In the wintertime, on the other hand, large increases in *P* and more muted changes in *E* in the same NH middle- and high-latitude regions, lead to an extensive *P-E* anomaly (Figure 3). This is associated with an increase in both surface and 3 m soil moisture (Figure 4). In contrast to summertime drying, infiltration, by wetting the soil and increasing hydraulic conductivity, enhances downward transport of the extra precipitation under the influence of gravity, communicating the wetting to deeper soil layers. This increase in deeper soil moisture carries over to the rest of the year and is reflected in the annual mean (Figure 2). In summary, we interpret the contrasting changes in Figures 1 and 2 between surface and total soil moisture in northern middle and high latitudes as resulting from differing seasonal *P* and *E* responses (increased wintertime precipitation and increased summertime evaporation) in conjunction with the fundamental soil physical asymmetry between infiltration and evaporation processes. The contrast between overall summer drying and winter wetting in these regions has been noted before [*Milly*, 1997; *Wetherald and Manabe*, 2002; *Wang*, 2005]; here we show that it is associated with a negative gradient of annual soil moisture changes down from the surface. This also explains how extensive surface drying, in the annual mean, can occur in the absence of a significant annual *P-E* anomaly (Figure 3) [e.g., *Swann et al.*, 2016].

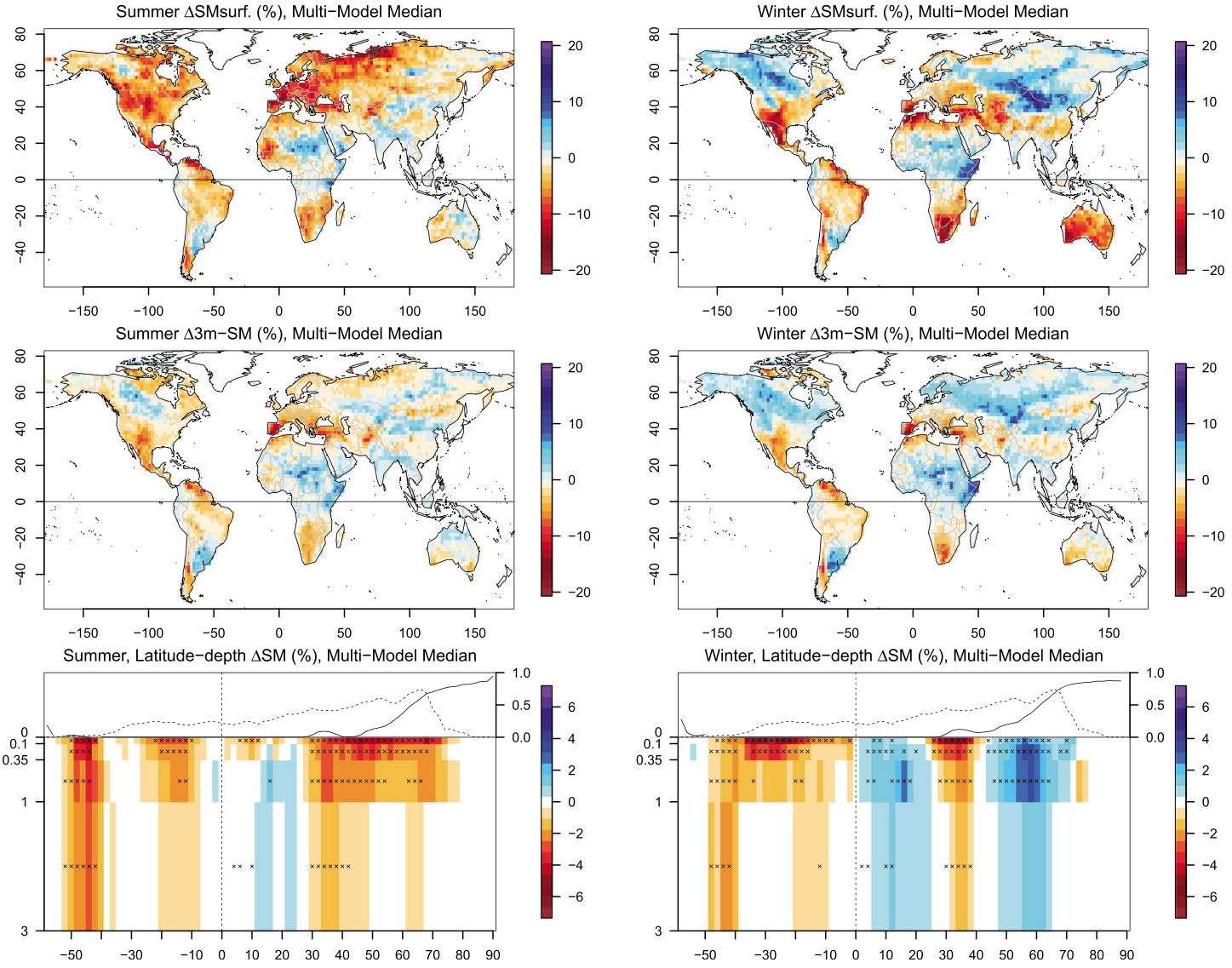

Figure 4. Multimodel median relative change (%) in (left) summer and (right) winter (top row) surface soil moisture, (middle row) 3 m soil moisture, and zonal-depth soil moisture. Summer is JJA in the Northern Hemisphere and DJF in the Southern Hemisphere and vice versa for winter. (bottom) Similar as in Figure 2.

Figure S5 highlights the differences in winter and summer zonal mean changes between three broad longitudinal bands. It confirms, in more details, that the pattern of summertime surface drying and wintertime recharge over different regions is in qualitative agreement with zonal *P-E* changes. There is, again, a pronounced contrast between changes in *P-E* and soil moisture over Central America, which remain negative throughout the year, and changes over tropical Africa, which exhibit pronounced winter (and fall; not shown) increases in *P-E* and soil moisture. Note that in the Southern Hemisphere (SH), the most intense surface drying tends to occur in the (austral) winter approximately 30°S (e.g., South Africa and Australia; Figure 4), symmetrical to wintertime drying in the NH around 30°N. The SH lacks land at higher latitudes (40–60°S) where summertime drying similar to the NH would presumably occur.

Overall, our analysis supports recent research arguing that future drought and aridity projections should be based directly on climate model simulations of the water cycle rather than based on off-line metrics computed a posteriori [*Roderick et al.*, 2015; *Milly and Dunne*, 2016; *Swann et al.*, 2016]. Indeed, the negative vertical gradient of soil moisture changes identified in our results implies that the extensive drying predicted by off-line metrics, while consistent with projected decline in surface soil moisture, will tend to overestimate (negatively) total changes in soil water availability. Changes in total or 3 m soil moisture, as a result of the

processes discussed above, appear to remain essentially constrained by changes in mean annual precipitation (Figures 1 and 3). They remain much less negative than drought metric changes, suggesting more nuanced changes in water resources. Consistent with our results, *Cheng et al*. [2016], for instance, recently found different qualitative impacts of global warming on California drought when considering different soil moisture depths: diagnoses based on surface soil moisture lead to projections of increased drought occurrence, while those based on 1 m soil moisture lead to decreased drought occurrence. This also suggests more nuanced impacts on agricultural and natural ecosystems, especially with respect to vegetation types able to extract water from deeper soil layers (in their review of more than 250 species, *Canadell et al*. [1996] indicate that the average maximum rooting depth around the globe is 4.6 m). We point out that climate models generally project increased vegetation cover around most of the globe, including middle to high northern latitudes, suggesting that vegetation may be able to develop despite summertime drying [*Mahowald et al*., 2016].

Finally, the vertical gradient of soil moisture change identified in our analysis highlights the importance of vertical soil water transport processes in climate models, as well as that of evapotranspiration processes that can affect soil moisture at different levels. For instance, the partitioning of E into soil evaporation, canopy-intercepted water evaporation, and plant transpiration varies largely between models and remains poorly constrained by observations on a global scale. While some of the intermodel uncertainty in soil moisture changes can be ascribed to differences in climate change patterns in each model [e.g., *Orlowsky and Seneviratne*, 2013], the diversity of model soil schemes and soil and vegetation parameterizations arguably plays some role in the model spread in spatial and vertical patterns of soil moisture change. Reducing this structural uncertainty, as well as improving the representation of soil depth and soil hydraulic properties in land models [e.g., *Hengl et al*., 2014], could be essential to provide more robust projections of future changes in soil water availability and more generally of changes in the terrestrial water cycle.

5. Conclusion

We investigated future soil moisture changes at different depths in CMIP5 projections, making use of layer-by-layer soil moisture outputs that were for the first time reported in CMIP5. Our results indicate a vertical pattern of projected soil moisture changes under global warming, with a negative gradient from the surface downward. As a result, multimodel projections of surface soil moisture changes show more extensive and larger decreases than changes in soil moisture integrated over the first 3 m. We identify regions of decreased annual surface soil moisture but increased 3 m soil water (northern U.S./central Canada and central Asia). The vertical pattern of soil moisture changes is qualitatively consistent with a picture of enhanced evaporative demand drying surface soil moisture, but total changes in water content remaining dominated by precipitation changes. Our results shed some light on the apparent discrepancy between the extensive drying predicted by off-line aridity and drought metrics focusing on conditions of the near-surface atmosphere and the more modest changes predicted from changes in the water budget: the former mostly affects surface soil moisture, while the latter are reflected in column-integrated soil moisture. These different behaviors need to be taken into account when inferring impacts of climate change on water resources and agriculture.

Acknowledgments
This study was supported by NOAA project NA15OAR4310091. We acknowledge the World Climate Research Programme's Working Group on Coupled Modelling, which is responsible for CMIP, and we thank the climate modeling groups (listed in Table S1 of this paper) for producing and making available their model output. For CMIP the U.S. Department of Energy's Program for Climate Model Diagnosis and Intercomparison provides coordinating support and led development of software infrastructure in partnership with the Global Organization for Earth System Science Portals.

References

Berg, A., et al. (2016), Land-atmosphere feedbacks amplify aridity increase over land under global warming, *Nat. Clim. Change*, doi:10.1038/nclimate3029.
Burke, E. J., S. J. Brown, and N. Christidis (2006), Modeling the recent evolution of global drought and projections for the twenty-first century with the Hadley Centre climate model, *J. Hydrometeorol.*, *7*, 1113–1125.
Canadell, J., R. B. Jackson, J. B. Ehleringer, H. A. Mooney, O. E. Sala, and E. D. Schulze (1996), Maximum rooting depth of vegetation types at the global scale, *Oecologia*, *108*(4), 583–595.
Cheng, L., M. Hoerling, A. AghaKouchak, B. Livneh, X. W. Quan, and J. Eischeid (2016), How has human-induced climate change affected California drought risk?, *J. Clim.*, *29*(1), 111–120.
Collins, M., et al. (2013), Long-term climate change: Projections, commitments and irreversibility, in *Climate Change 2013: The Physical Science Basis. Contribution of Working Group I to the Fifth Assessment Report of the Intergovernmental Panel on Climate Change*, edited by T. F. Stocker et al., Cambridge Univ. Press, Cambridge, U. K., and New York.
Cook, B. I., J. E. Smerdon, R. Seager, and S. Coats (2014), Global warming and 21st century drying, *Clim. Dyn.*, *43*, 2607–2627.
Dai, A. (2013), Increasing drought under global warming in observations and models, *Nat. Clim. Change*, *3*(1), 52–58.
Feng, S., and Q. Fu (2013), Expansion of global drylands under a warming climate, *Atmos. Chem. Phys.*, *13*, 10,081–10,094.
Fu, Q., and S. Feng (2014), Responses of terrestrial aridity to global warming, *J. Geophys. Res. Atmos.*, *119*, 7863–7875.
Hengl, T., et al. (2014), SoilGrids 1 km—Global soil information based in automated mapping, *PLoS One*, *9*, e105992.

Hoerling, M. P., J. K. Eischeid, X. W. Quan, H. F. Diaz, R. S. Webb, R. M. Dole, and D. R. Easterling (2012), Is a transition to semipermanent drought conditions imminent in the US Great Plains?, *J. Clim.*, *25*(24), 8380–8386.

Huang, J., H. Yu, X. Guan, G. Wang, and R. Guo (2016), Accelerated dryland expansion under climate change, *Nat. Clim. Change*, *6*(2), 166–171, doi:10.1038/nclimate2837.

Koster, R. D., Z. Guo, R. Yang, P. A. Dirmeyer, K. Mitchell, and M. J. Puma (2009), On the nature of soil moisture in land surface models, *J. Clim.*, *22*(16), 4322–4335.

Koven, C. D., W. J. Riley, and A. Stern (2013), Analysis of permafrost thermal dynamics and response to climate change in the CMIP5 Earth system models, *J. Clim.*, *26*, 1877–1900.

Lawrence, D. M., C. D. Koven, S. C. Swenson, W. J. Riley, and A. G. Slater (2015), Permafrost thaw and resulting soil moisture changes regulate projected high-latitude CO_2 and CH_4 emission, *Environ. Res. Lett.*, *10*(9), 094,011.

Lin, L., A. Gettelman, S. Feng, and Q. Fu (2015), Simulated climatology and evolution of aridity in the 21st century, *J. Geophys. Res. Atmos.*, *120*, 5795–5815.

Mahowald, N., F. Lo, Y. Zheng, L. Harrison, C. Funk, D. Lombardozzi, and C. Goodale (2016), Projections of leaf area index in Earth system models, *Earth Sys. Dyn.*, *7*, 211–229.

Milly, P. C. (1997), Sensitivity of greenhouse summer dryness to changes in plant rooting characteristics, *Geophys. Res. Lett.*, *24*(3), 269–271, doi:10.1029/96GL03968.

Milly, P. C., K. A. Dunne, and A. V. Vecchia (2005), Global pattern of trends in streamflow and water availability in a changing climate, *Nature*, *438*(7066), 347–350.

Milly, P. C. D., and K. A. Dunne (2016), Potential evapotranspiration and continental drying, *Nat. Clim. Change*, doi:10.1038/nclimate3046.

Orlowsky, B., and S. I. Seneviratne (2013), Elusive drought: Uncertainty in observed trends and short- and long-term CMIP5 projections, *Hydrol. Earth Syst. Sci.*, *17*, 1765–1781.

Roderick, M. L., P. Greve, and G. D. Farquhar (2015), On the assessment of aridity with changes in atmospheric CO_2, *Water Resour. Res.*, *51*, 5450–5463, doi:10.1002/2015WR017031.

Scheff, J., and D. M. W. Frierson (2014), Scaling potential evapotranspiration with greenhouse warming, *J. Clim.*, *27*, 1539–1558.

Scheff, J., and D. M. W. Frierson (2015), Terrestrial aridity and its response to greenhouse warming across CMIP5 climate models, *J. Clim.*, *28*, 5583–5600.

Sheffield, J., and E. F. Wood (2008), Projected changes in drought occurrence under future global warming from multi-model, multi-scenario, IPCC AR4 simulations, *Clim. Dyn.*, *1*, 79–105.

Swann, A., F. M. Hoffman, C. D. Koven, and J. T. Randerson (2016), Plant responses to increasing CO_2 reduce estimates of climate impacts on drought severity, *Proc. Natl. Acad. Sci. U.S.A.*, doi:10.1073/pnas.1604581113.

Wang, G. L. (2005), Agricultural drought in a future climate: Results from 15 global climate models participating in the IPCC 4th assessment, *Clim. Dyn.*, *25*, 739–753.

Wetherald, R. T., and S. Manabe (2002), Simulation of hydrologic changes associated with global warming, *J. Geophys. Res.*, *107*(D19), 4379, doi:10.1029/2001JD001195.

Zhao, T., and A. Dai (2015), The magnitude and causes of global drought changes in the 21st century under a low-moderate emissions scenario, *J. Clim.*, *28*(11), 4490–4512.